



Mineralogical Characterization and Firing Technology of Ancient Ceramics through XRD: A Case Study from Jalandhar District, Punjab (India)

Rahul Kumar^{*1}  Narender Parmar¹  and Jitendra Kumar Pattanaik² 

**Corresponding Author; ¹Department of History and Archaeology Central University of Haryana, Mahendergarh, India.
E- mail:Rahul200300@cuh.ac.in*

²Department of Geology School of Environment and Earth Sciences Central University of Punjab, Punjab, India.

Received: 04/ 02/ 2026; Received in Revised form: 27/ 04/ 2026; Accepted: 23/ 05/ 2026 Published: 20/ 06/ 2026

Abstract

Ceramic artefacts constitute one of the most reliable material indicators for reconstructing technological traditions, cultural behaviour, and patterns of resource utilisation in ancient societies. The present study undertakes a mineralogical and phase-based characterisation of pottery samples recovered from four recently explored archaeological sites in the Jalandhar Doab region of Punjab, namely Kathpalon, Goal Pind, Hardo Pharla, and Singhpur. A total of forty representative samples, spanning the Late Harappan to Early Medieval periods (c. 2000 BCE–1200 CE), were analysed using X-ray diffraction (XRD) to identify crystalline mineral phases and to infer firing conditions and clay provenance. The results indicate that the ceramics were predominantly fired under low- to moderate-temperature regimes, ranging approximately between 500 °C and 900 °C, under both oxidising and reducing atmospheric conditions. The persistence of minerals such as quartz and calcite, together with the occurrence of dickite and phlogopite in certain samples, suggests variability in firing intensity and technological control across different cultural phases. Although firing temperatures appear broadly consistent through time, variations in mineralogical assemblages point to changes in clay source procurement, reflecting evolving potting traditions and experimentation by craftspeople in the region. This study highlights the effectiveness of XRD-based mineralogical analysis in reconstructing ancient ceramic technology, while recognising that further microstructural investigations (e.g. SEM analysis) would enhance understanding of amorphous phases and vitrification processes.

Keywords: XRD Analysis, Mineralogical Phases, Ceramic Technology, Firing Temperature, Jalandhar Doab.

Article Type: Research Article

Introduction

Pottery represents one of the most durable and informative categories of archaeological evidence, offering valuable insights into the technological knowledge, cultural practices, and economic organisation of past societies. Earlier archaeological approaches primarily emphasised typology and stylistic attributes; however, the incorporation of scientific analytical methods has significantly expanded our understanding of ceramic production, particularly with regard to raw material selection, firing technology, and functional performance.

X-ray diffraction (XRD) has emerged as a key archaeometric technique for identifying crystalline mineral phases in ceramic materials, enabling researchers to reconstruct firing conditions, clay composition, and thermal transformations. In the Indian context, several studies have applied XRD to Harappan and post-Harappan ceramics, demonstrating its utility in reconstructing production technologies and firing regimes. Despite this, the ceramic traditions of the Jalandhar Doab region remain comparatively underexplored from a scientific perspective, notwithstanding the region's archaeological richness and cultural continuity.



The present study seeks to address this lacuna through a systematic mineralogical investigation of pottery samples collected from four archaeological sites in Jalandhar district: Kathpalon (31°01'54" N, 75°50'55" E), Goal Pind (31°26'12" N, 75°40'40" E), Hardo Pharla (31°14'32" N, 75°39'31" E), and Singhpur (31°31'20" N, 75°36'48" E). Collectively, these sites represent a diachronic cultural sequence extending from the Late Harappan to the Early Medieval period (Rahul 2024: 3-6). The specific objectives of the study are to examine:

- the mineralogical phases present in the ceramics and their technological implications
- firing temperature ranges and kiln atmosphere conditions
- variations in clay procurement across cultural periods.

Unlike earlier studies that rely predominantly on typological analysis, this research integrates scientific data with archaeological interpretation to provide a more comprehensive understanding of ancient pottery production in the Punjab region.

Materials and Methods

Forty pottery samples representing a range of ceramic categories, including fine red ware, black-slipped ware, coarse grey ware, fine grey ware, and red ware, were selected from surface collections and field surveys conducted at the four study sites. Care was taken to ensure stratigraphic and chronological representation across different cultural phases.

Powdered samples were prepared following standard archaeological sampling protocols. X-ray diffraction analysis was carried out using a PANalytical Empyrean diffractometer with CuK α radiation ($\lambda = 0.15408$ nm), operated at 45 kV and 40 mA. Diffractograms were recorded over a 2θ range of 5°–90° under ambient conditions. Phase identification was undertaken using JCPDS/ICDD reference standards, following established guidelines for XRD interpretation.

It should be noted that XRD identifies only crystalline mineral phases and does not yield direct information on microstructural features or amorphous phases. Although SEM-based analysis would permit more detailed microstructural interpretation, the present study is confined to phase-based mineralogical characterisation, which nonetheless provides a robust basis for reconstructing firing regimes and technological choices.

In total, forty samples were analysed from the archaeological sites of Kathpalon (KPL), Goal Pind (GPD), Hardo Pharla (HPL), and Shingpura (SPR) (Figure. 1). The different ceramic varieties examined, including fine red ware, black-slipped ware, coarse grey ware, fine grey ware, and red ware, are illustrated in (Figure. 2a-d).

Instrumentation and XRD Analysis

Powder X-ray diffraction (XRD) analysis was carried out on powdered pottery samples using an Empyrean PANalytical diffractometer at the Inter

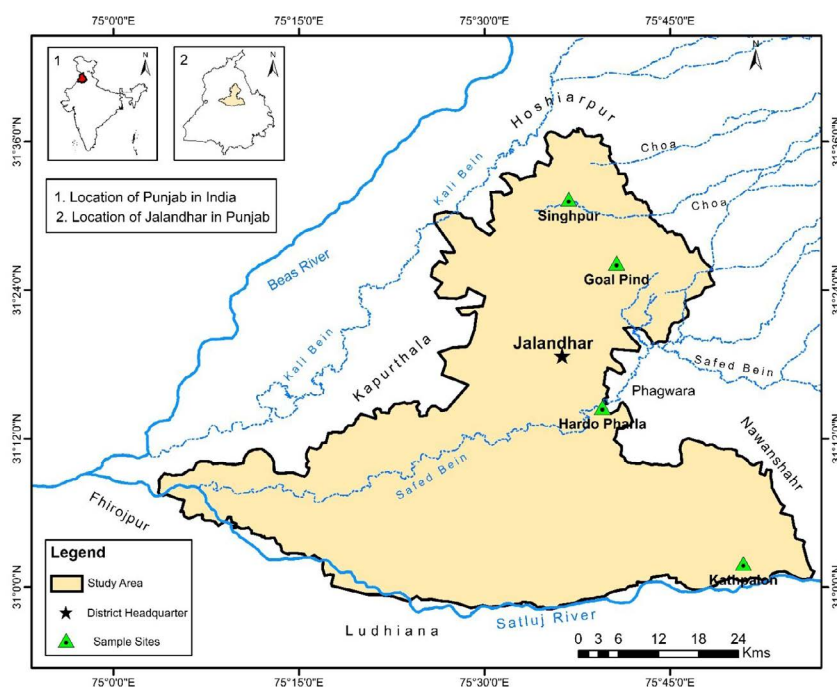


Figure 1: Map of the Sample Sites.

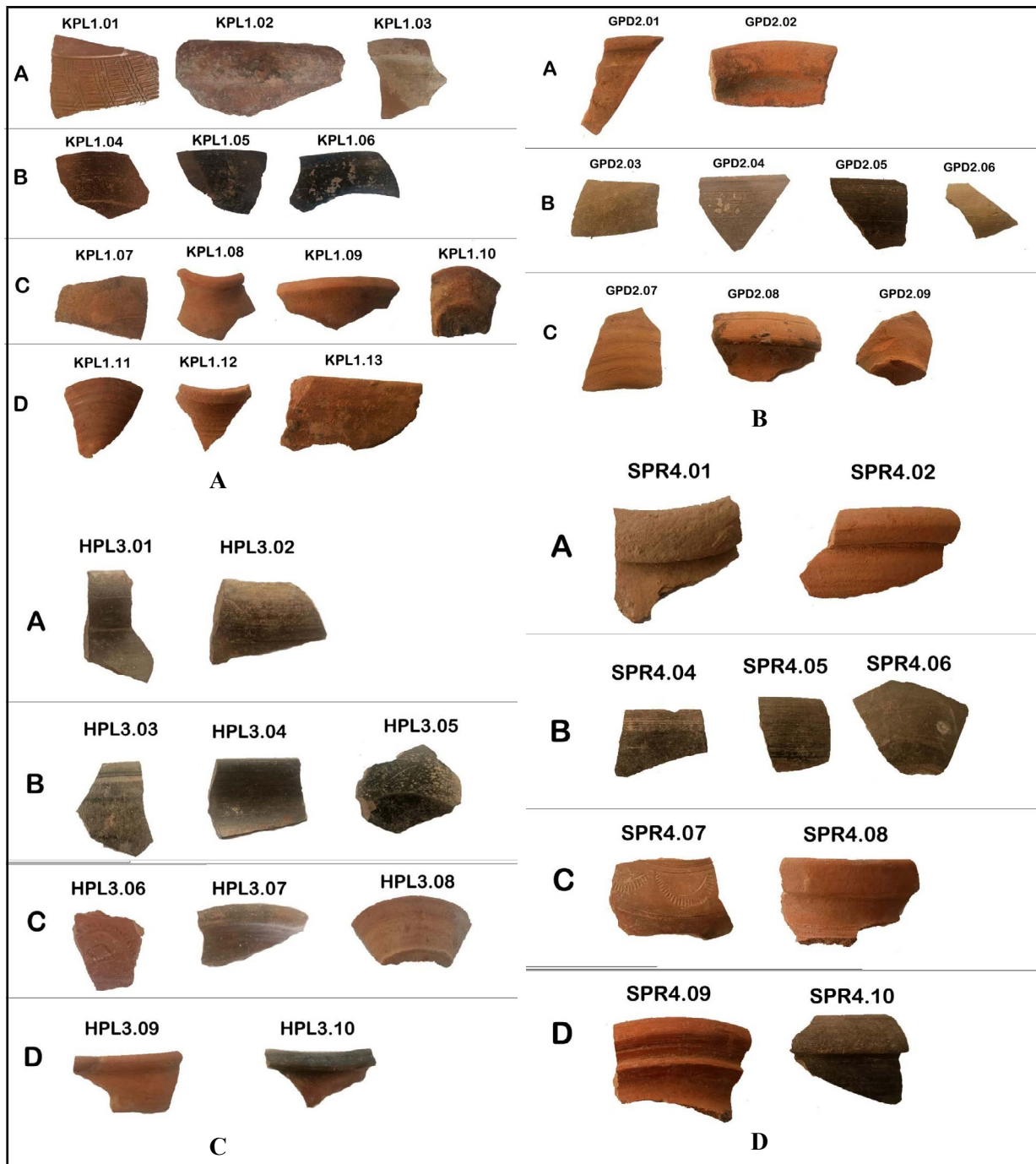


Figure 2: (A) KPL: A (Late Harappan), B (Early Historical), C (Historical), D (Early Medieval). (B) GPD: A (Late Harappan), B (Early Historical), C (Historical). (C) HPL: A (Late Harappan), B (Early Historical), C (Historical), D (Early Medieval). (D) SPR: A (Late Harappan), B (Early Historical), C (Historical), D (Early Medieval).

University Accelerator Centre (IUAC), Delhi. The analysis employed $\text{CuK}\alpha$ radiation ($\lambda = 0.15408$ nm), generated at an operating voltage of 45 kV and a current of 40 mA, to determine the mineralogical phases present in the ceramic fabrics.

X-ray diffractograms were recorded at room temperature over a 2θ range of 5° – 90° , with a scan

step size of 0.0167° and a total scan time of 34.925 minutes per sample. These parameters were selected to ensure accurate identification of crystalline phases within the clay minerals. Mineralogical interpretation followed established protocols for XRD analysis (Bish 1989: 19–25).

The Malvern PANalytical system incorporates advanced hybrid detector technology and is equipped with a flat sample stage for mounting powdered specimens, along with an MPSS (multi-purpose sample stage), facilitating precise and reproducible measurements. Identification of crystalline mineral phases was undertaken using the Joint Committee on Powder Diffraction Standards (JCPDS) database (Berry 1974). This database includes the Powder Diffraction File (PDF), which compiles reference diffraction patterns and is widely recognised as the standard reference source for XRD-based mineral identification.

XRD analysis operates on the principle that incident waves interact with periodic atomic structures, producing diffraction effects when the wavelength of the radiation corresponds to the periodicity of the crystal lattice. In crystallographic investigations, electrons or neutrons of appropriate energy, as well as X-rays with wavelengths comparable to unit cell dimensions, are employed to obtain diagnostic diffraction patterns.

Results and Interpretation

Across all four archaeological sites, quartz was identified as the most ubiquitous mineral phase, confirming its role as a primary constituent of the ceramic fabric. The presence of calcite, mica (phlogopite), feldspar (albite), rutile, and clay minerals such as dickite reflects a diverse range of mineralogical assemblages, indicative of both technological choices and the inherent composition of locally available clay sources.

Late Harappan ceramic assemblages generally suggest firing within a moderate temperature range of approximately 550–900 °C, often under reducing atmospheric conditions, as indicated by the presence of graphite and magnetite phases. In contrast, Early Historical and Historical ceramics exhibit more refined control over firing regimes, with carefully regulated oxidising and reducing conditions producing distinct ware types, including red-slipped and black-slipped pottery.

Samples from Kathpalon and Hardo Pharla reveal continuity in clay mineral composition across certain cultural phases, implying consistent raw material procurement strategies. Conversely, notable variations observed in Early Medieval wares suggest subsequent shifts in clay sourcing practices. At

Goal Pind and Singhpur, the presence of dickite and untransformed calcite in selected samples points to relatively low firing temperatures and deliberate technological constraints in ceramic production.

Major diffraction peaks were observed at characteristic 2θ values in samples from Kathpalon (KPL) (Table 1), Goal Pind (GPD) (Table. 2), Hardo Pharla (HPL) (Table. 3), and Singhpur (SPR) (Table. 4), as illustrated in the corresponding diffractograms. Collectively, these results indicate that potters in the Jalandhar Doab region possessed a nuanced understanding of ceramic production, demonstrating experimentation with firing techniques, clay sources, and surface treatments across successive cultural periods.

The data given in the tables has been analyzed by the Geology Department Lab, Central University of Punjab (Bathinda, India). This is based on the XRD analysis, which was done in the Geochronology Lab, IUAC (Delhi, India) on 16/05/2024.

Description of Possible Minerals in Pottery Samples of Kathpalon Site.

The major mineralogical composition of the pottery samples was determined using an X-ray diffractometer. Identification of crystalline mineral phases was carried out with reference to the JCPDS database. A summary of the mineral assemblages identified in the pottery samples is presented in Table 1, while the corresponding diffraction patterns are illustrated in Figure 3a. Quartz, calcite, mica (phlogopite), albite, and iron oxides occur in almost all analysed samples.

The Late Harappan pottery samples (KPL1.01–KPL1.03) exhibit several prominent 2θ diffraction peaks, as identified from the XRD patterns. Based on peak intensities, the corresponding mineral phases include quartz (SiO_2), constituting approximately 30–50% and indicating a dominant silica content; calcite (CaCO_3) at 5–10%; mica (phlogopite) [$\text{K}(\text{Mg},\text{Fe})_3(\text{Al},\text{Fe})\text{Si}_3\text{O}_{10}(\text{OH},\text{F})_2$] at 7–16%; bloedite [$\text{Na}_2\text{Mg}(\text{SO}_4)_2 \cdot 4\text{H}_2\text{O}$] at 9–17%; feldspar (plagioclase/albite) at approximately 14%; and minor phases such as rutile, graphite, and spinel, each contributing around 1%. Additional minor minerals, including diopside and dolomite, are also present.

In the Early Historical period samples (KPL1.04–KPL1.06), the dominant mineral phases comprise quartz (SiO_2) at 42–76%, calcite (CaCO_3) at approx-

imately 4%, mica (phlogopite) at 10–12%, fluorite at 3%, rutile at 3%, graphite at 5%, and spinel at 3%. Covellite is notably present at 23% in sample KPL1.06. Feldspar (plagioclase/albite) occurs in the range of 16–18%, while muscovite constitutes approximately 12% in sample KPL1.04.

The Historical period samples (KPL1.07–KPL1.10) are characterised by quartz (SiO_2) contents ranging from 40–68%, calcite (CaCO_3) from 2–17%, and mica (phlogopite) at approximately 21%. Other identified minerals include fluorite at 4%, rutile at 1–5%, graphite at 20% in sample KPL1.09, feldspar (plagioclase/albite) at 20–23%, sodalite at 2%, and muscovite at approximately 11%. Minor mineral constituents such as garnet (almandine), pseudoeucryptite, palygorskite, and pyroxene (clinostatite) are also present within this assemblage.

The Early Medieval pottery samples (KPL1.11–KPL1.13) display quartz (SiO_2) contents of approximately 45–53%, again indicating a dominant silica component. Calcite (CaCO_3) occurs at around 2%, while mica (phlogopite) ranges between 21–30%. Rutile is present at approximately 1%, graphite at around 5%, feldspar (plagioclase/albite) at 13%, and the clay mineral dickite at approximately 11%. Minor mineral phases identified in these samples include anatase and garnet (almandine).

Description of Possible Minerals in Pottery Samples of Goal Pind Site

Table 2 includes a summary of the mineral assemblage of the pottery samples of Goal Pind site, and the corresponding diffraction patterns are shown in Figure 3b. Quartz, Calcite, Mica (Phlogopite), Rutile, Fluorite, Hematite, and Albite are present in the samples. The Late Harappan pottery sample GPD2.01-2.02 displays the following significant 2θ diffraction peaks identified from the XRD graph. Their corresponding minerals based on peak intensities, include: Quartz (SiO_2) – 30–45%, Calcite (CaCO_3) 1%, Mica (Phlogopite) ($\text{K}(\text{Mg}, \text{Fe})^3(\text{Al}, \text{Fe})\text{Si}_3\text{O}_{10}(\text{OH}, \text{F})^2$) 12–20%, Rutile 3–11%, Fluorite 3%, Hematite 2% and Feldspar (Plagioclase/Albite) – 26–33%. Minor Minerals are Zircon, Chalcopyrite, and Pseudoeucryptite, also present in these samples. The pottery colour redish by the presence of hematite. In the samples of the Early Historical period (GPD2.03–2.06), the major minerals are Quartz (SiO_2) – 42–60%, Calcite (CaCO_3) 3% (GPD2.04), Mica (Phlogopite) ($\text{K}(\text{Mg}, \text{Fe})^3(\text{Al}, \text{Fe})\text{Si}_3\text{O}_{10}(\text{OH}, \text{F})^2$) 12–20%, Rutile 2–5%, Graphite 8–35%, Covellite 23% (KPL1.06), Feldspar (Plagioclase/Albite) – 8–25%, Muscovite 14% (GPD1.04), and Sodalite 2% (GPD2.05). Minor minerals like Libethenite, Halite, Hercynite, Pseudoeucryptite, Garnet (Pyrope), and Dyscrasite

Table 1: Possible Minerals in Kathpalon (KPL) Site Samples.

Cul.	Sam.	Qu.	Fl.	Cal.	M.P.	Blo.	Tri.	Ru.	Gr.	Sp.	Ber.	C.M.	So.	M.M	Pla.	Co.	Tem.
L.H	KPL1.01	+	+	+	+	+											550-900°C
	KPL1.02	+		+	+		+	+					+				
	KPL1.03	+		+	+	+			+	+					+	+	
E.H	KPL1.04	+		+			+	+	+					+	+		600-900°C
	KPL1.05	+	+		+			+		+							
	KPL1.06	+			+											+	
H	KPL1.07	+	+	+				+						+	+		600-850°C
	KPL1.08	+	+	+			+	+									
	KPL1.09	+	+	+	+		+		+		+						
	KPL1.10	+						+			+		+		+		
E.M	KPL1.11	+		+	+		+	+							+		600-850°C
	KPL1.12	+			+		+		+		+	+					Below 650°C
	KPL1.13	+	+		+			+				+					

Cul: Culture; **Sam:** Sample Code; **Qu:** Quartz; **Fl:** Fluorite; **Cal:** Calcite; **M.P:** Mica (Phlogopite); **Blo:** Bloeditite; **Tri:** Tridymite (High temp. Quartz); **Ru:** Rutile; **Gr:** Graphite; **Sp:** Spinel; **Ber:** Berlinite; **C.M:** Clay mineral (Dickite); **So:** Sodalite; **M.M:** Mica (Muscovite); **Pla:** Plagioclase (Albite); **Co:** Covellite; **Tem:** Temperature.

L.H: Late Harappan; **E.H:** Early Historical; **H:** Historical; **E.M:** Early Medieval.

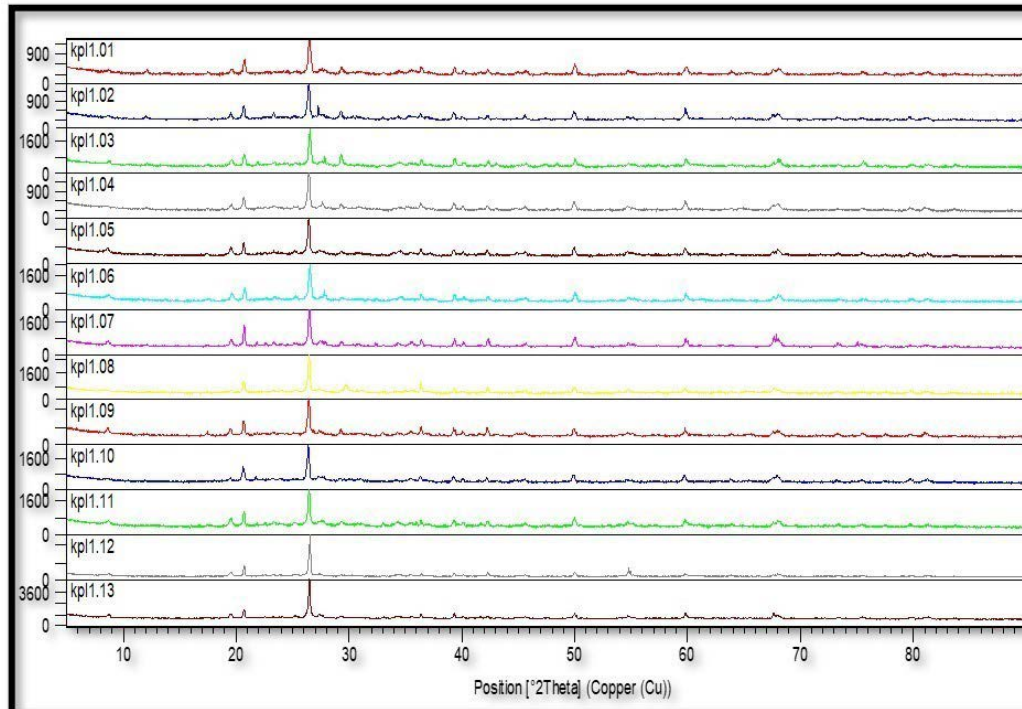


Figure. 3a: XRD Graph of Kathpalon (KPL) Site Samples. (After: Geochronology Lab. IUAC. Delhi. India)

are also present in pottery samples. In the samples of the Historical period (GPD2.07-GPD2.09), the major minerals are Quartz (SiO_2) – 45-70%, Mica (Phlogopite) ($\text{K}(\text{Mg}, \text{Fe})^3(\text{Al}, \text{Fe})\text{Si}_3\text{O}_{10}(\text{O}, \text{H}, \text{F})^2$) 13%, Fluorite 4%, Rutile 2%, Graphite 5% (GPD2.08), Feldspar (Plagioclase/Albite) – 8%, Muscovite 8%, Biotite 28% (GPD2.09), and Clay mineral Dickite 6% (GPD2.07). Minor minerals Marshite, Senarmontite, Libethenite, Titanite, Akermanite, Brucite deuterated, Lepidolite, Pyroxene (Protoenstatite), Pseudoeucryptite, and Anatase, are also present in pottery.

Description of Possible Minerals in Pottery Samples of Hardo Pharla Site

Table 3 includes a summary of the mineral assemblage of the pottery samples (Hardo Pharla site), and the corresponding diffraction patterns are shown in Figure 3c. Quartz, Rutile, Fluorite, Graphite, Calcite, Mica (Phlogopite), Albite, and Clay mineral (Dickite) are present in the samples. The Late Harappan pottery sample HPL3.01-3.02 displays the following significant 2θ diffraction peaks, identified from the XRD graph, and their corresponding minerals, based on peak intensities, include: Quartz

Table. 2: Possible Minerals in Goal Pind (GPD) Site Samples.

Cul.	Sam.	Qu.	Fl.	Cal.	M.P	Tri.	Ru.	Gr.	C.M.	M.M.	Pla.	So.	Hem.	Bio	Tem.
L.H	GPD2.01	+	+	+	+	+	+				+				600-850°C
	GPD2.02	+	+		+		+				+		+		
E.H	GPD2.03	+				+	+	+							600-900°C
	GPD2.04	+		+		+	+	+		+					
	GPD2.05	+			+	+	+	+			+	+			
	GPD2.06	+			+		+				+				
H	GPD2.07	+							+	+	+				Below 650°C
	GPD2.08	+	+				+	+							550-850°C
	GPD2.09	+			+						+			+	

Cul: Culture; **Sam:** Sample Code; **Qu:** Quartz; **Fl:** Fluorite; **Cal:** Calcite; **M.P:** Mica (Phlogopite); **Tri:** Tridymite (High temp. Quartz); **Ru:** Rutile; **Gr:** Graphite; **C.M:** Clay mineral (Dickite); **M.M:** Mica (Muscovite); **Pla:** Plagioclase (Albite); **So:** Sodalite; **Hem:** Hematite; **Bio:** Biotite; **Tem:** Temperature.

L.H: Late Harappan; **E.H:** Early Historical; **H:** Historical.

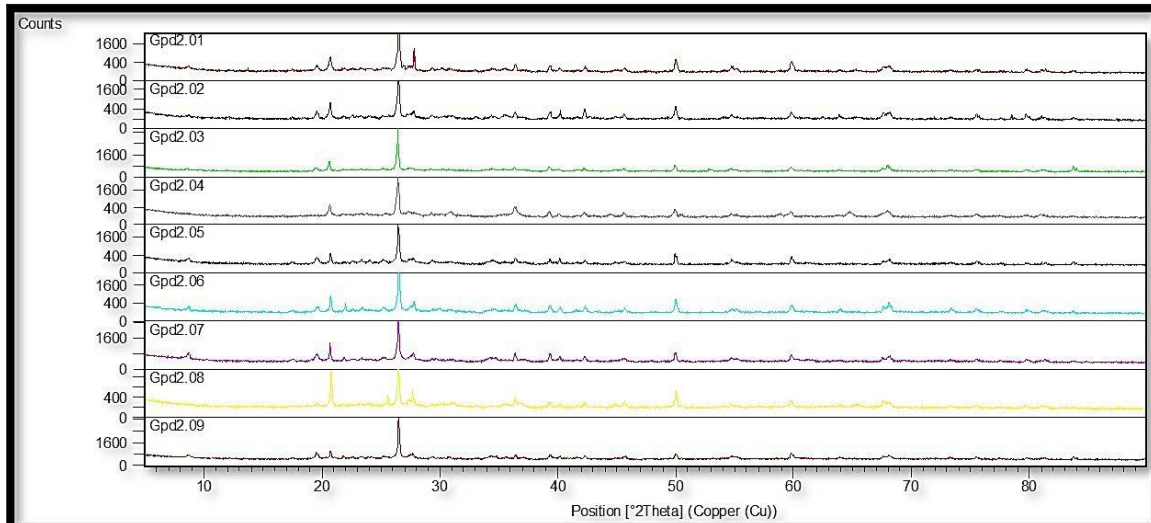


Figure 3b: XRD Graph of Goal Pind (GPD) Site Samples (After: Geochronology Lab. IUAC. Delhi. India)

(SiO₂) – 58-87%, indicating a dominant silica content, Fluorite 4%, Rutile 2-4%, and Graphite 9%. Minor minerals, such as tellurobismuth, Carlinite, Cinnabar, Ankerite, Halite, and Pseudoeucryptite, are also present in pottery samples. In the samples of the Early Historical period (HPL3.03-3.05), the major minerals are Quartz (SiO₂) – 43-54%, Mica (Phlogopite) (K (Mg, Fe)³ (Al, Fe) Si₃ O₁₀ (O H, F)²) 16-19%, Rutile 3%, Graphite 7-31%, Brucite 4-6%, Bloedite 17 (HPL3.03), and Clay mineral (Dickite) 11% (HPL3.05). Minor minerals like Berlinite, Serpierite, Dyscrasite, Garnet (Almandine), Anatase Pyrope are also present. In the samples of the His-

torical period (HPL3.06-3.08), the major minerals are Quartz (SiO₂) – 53-74%, Calcite (CaCO₃) 4%, Mica (Phlogopite) (K (Mg, Fe)³ (Al, Fe) Si₃ O₁₀ (O H, F)²) 19%, Fluorite 2-4%, Rutile 2%, Sodalite 2-10%, and Protoenstatite 20% (3.07). Minor minerals Molybdite, Gaspeite, Chalcopyrite, Cebaite (Ce), Roquesite, Dyscrasite, and Polyolithionite are also present. In the samples of the Early medieval period (HPL3.09-3.10), the major minerals are Quartz (SiO₂) – 59-79%, Calcite (CaCO₃) 3%, Mica (Phlogopite) (K (Mg, Fe)³ (Al, Fe) Si₃ O₁₀ (O H, F)²) 11, Fluorite 3-8%, Rutile 2-5%, Graphite 6%, and Minor mineral Spinel, Dolomite also present.

Table 3: Possible Minerals in Hardo Pharla (HPL) Site Samples.

Cul.	Sam.	Qu.	Fl.	Cal.	M.P.	Tri.	Ru.	Gr.	C.M.	So.	Bru.	Tem.
L.H	HPL3.01	+				+	+	+				600-850°C
	HPL3.02	+	+			+	+					
E.H	HPL3.03	+					+	+			+	500-850°C
	HPL3.04	+			+	+	+				+	
	HPL3.05	+				+	+		+		+	Below 650°C
H	HPL3.06	+	+						+	+		Below 650°C
	HPL3.07	+	+		+							600-850°C
	HPL3.08	+	+	+			+			+		
E.M	HPL3.09	+	+		+		+					600-850°C
	HPL3.10	+	+	+		+	+	+				

Cul: Culture; Sam: Sample Code; Qu: Quartz; Fl: Fluorite; Cal: Calcite; M.P: Mica (Phlogopite); Tri: Tridymite (High temp. Quartz); Ru: Rutile;

Gr: Graphite; C.M: Clay mineral (Dickite); So: Sodalite; Bru: Brucite; Tem: Temperature.

L.H: Late Harappan; E.H: Early Historical; H: Historical; E.M: Early Medieval.

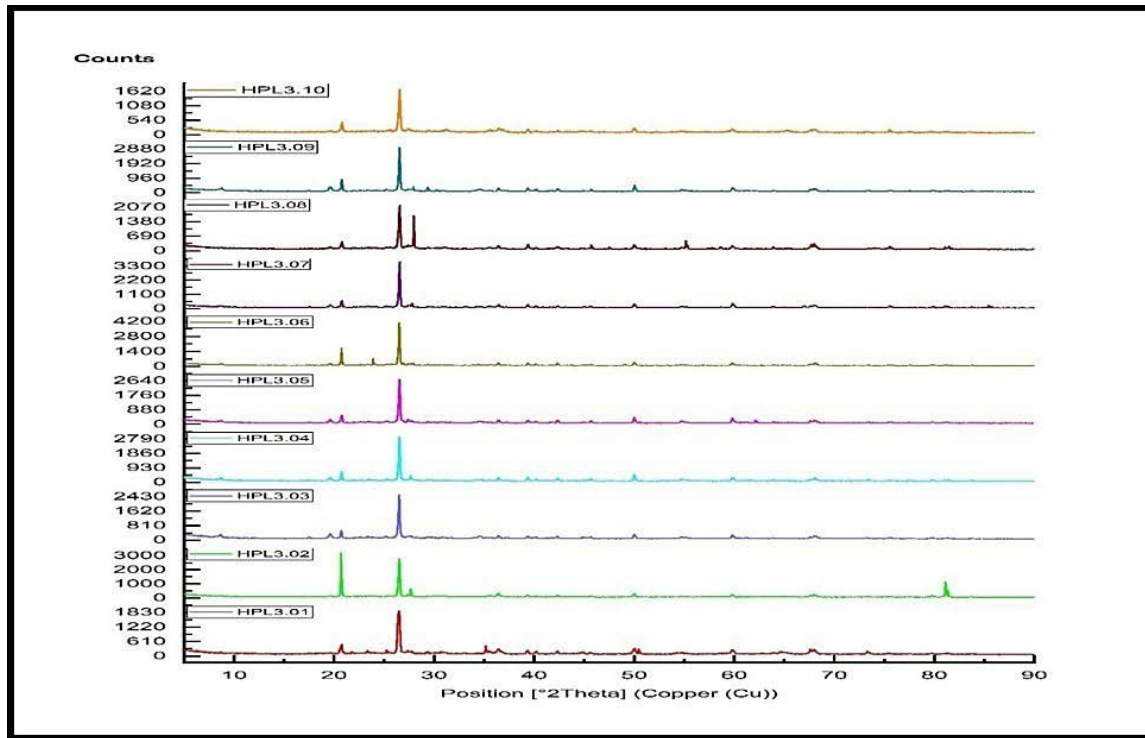


Figure 3c: XRD Graph of Hardo Pharla (HPL) Site Samples.

(After; Geochronology Lab. IUAC. Delhi. India)

Description of Possible Minerals in Pottery Samples of Singhpur Site

Table 4 includes a summary of the mineral assemblage of the pottery samples (Singhpur site), and the corresponding diffraction patterns are shown in Figure 3d. Quartz, Rutile, Covellite, Fluorite, Graphite, Calcite, Mica (Phlogopite), Albite, Pyroxene (Protoenstatite), and Clay mineral (Dickite) are present in the samples. The Late Harappan pottery sample SPR4.01-4.02 displays the following significant 2θ diffraction peaks identified from the XRD graph. Their corresponding minerals, based on peak intensities, include: Quartz (SiO_2) – 42-70% indicating dominant silica content, Fluorite 4%, Rutile 7%, Graphite 7%, Covellite 25%, Pyroxene (Protoenstatite) 14%, and Clay mineral (Dickite) 6%. Minor minerals like Gupeite, Baddeleyite, Tellurium, Calaverite, Nichromite are also present in pottery samples. In the samples of the Early Historical period (SPR4.04-4.06), the major minerals are Quartz (SiO_2) – 41-73%, Mica (Phlogopite) ($\text{K}(\text{Mg}, \text{Fe})^3(\text{Al}, \text{Fe})\text{Si}_3\text{O}_{10}(\text{OH}, \text{F})^2$) 17-20%, Graphite 3%, Covellite 10-17%, Pyroxene (Protoenstatite) 6%, and Calcite 2%. Minor minerals like Pseudoeu-

cryptite, Tapiolite, Lime, Bloedite, and Hercynite are also present. In the samples of the Historical period (SPR4.07-4.08), the major minerals are Quartz (SiO_2) – 60-80%, Calcite (CaCO_3) 4%, Fluorite 7%, Rutile 1%, Sodalite 2-5%, and Pyroxene (Protoenstatite) 6%. Minor minerals Anatase, Clinopyroxene, Pyrochlore (Gd-exchanged), Braunite, and Lime are also present. In the samples of the Early medieval period (SPR4.09), the major minerals are Quartz (SiO_2) – 52%, Calcite (CaCO_3) 2%, Mica (Phlogopite) ($\text{K}(\text{Mg}, \text{Fe})^3(\text{Al}, \text{Fe})\text{Si}_3\text{O}_{10}(\text{OH}, \text{F})^2$) 21, Fluorite 8%, Rutile 1%, and Pyroxene (Protoenstatite) 13%. Minor mineral Garnet (Almandine) is also present.

Discussion

The XRD patterns reveal the presence of minerals that underwent structural modifications during firing (heating) at varying temperatures (Cultrone *et al.* 2011: 345). The occurrence of kaolinite ($\text{Al}_2\text{Si}_2\text{O}_5(\text{OH})_4$) peaks in the samples suggests dehydroxylation processes taking place at approximately 450–600°C (Velraj *et al.* 2010: 92; Wu *et al.* 2013:

Table 4: Possible Minerals in Singhpur (SPR) Site Samples.

Cul.	Sam.	Qu.	Fl.	Cal.	M.P	Ru.	Gr.	C.M	Pla.	Co.	P.P.	Tem.
L.H	SPR4.01	+					+	+		+	+	Below 650°C
	SPR4.02	+	+			+						600-850°C
E.H	SPR4.04	+					+					600-800°C
	SPR4.05	+			+				+	+	+	
	SPR4.06	+		+	+					+		
H	SPR4.07	+	+	+					+			600-850°C
	SPR4.08	+	+					+				Below 650°C
E.M	SPR4.09	+	+	+	+						+	600-850°C

Cul: Culture; **Sam:** Sample Code; **Qu:** Quartz; **Fl:** Fluorite; **Cal:** Calcite; **M.P:** Mica (Phlogopite); **Ru:** Rutile; **Gr:** Graphite; **C.M:** Clay mineral (Dickite); **Pla:** Plagiocalsae (Albite); **Co:** Covellite; **P.P:** Pyroxene (Protoenstatite); **Tem:** Temperature.

L.H: Late Harappan; **E.H:** Early Historical; **H:** Historical; **E.M:** Early Medieval.

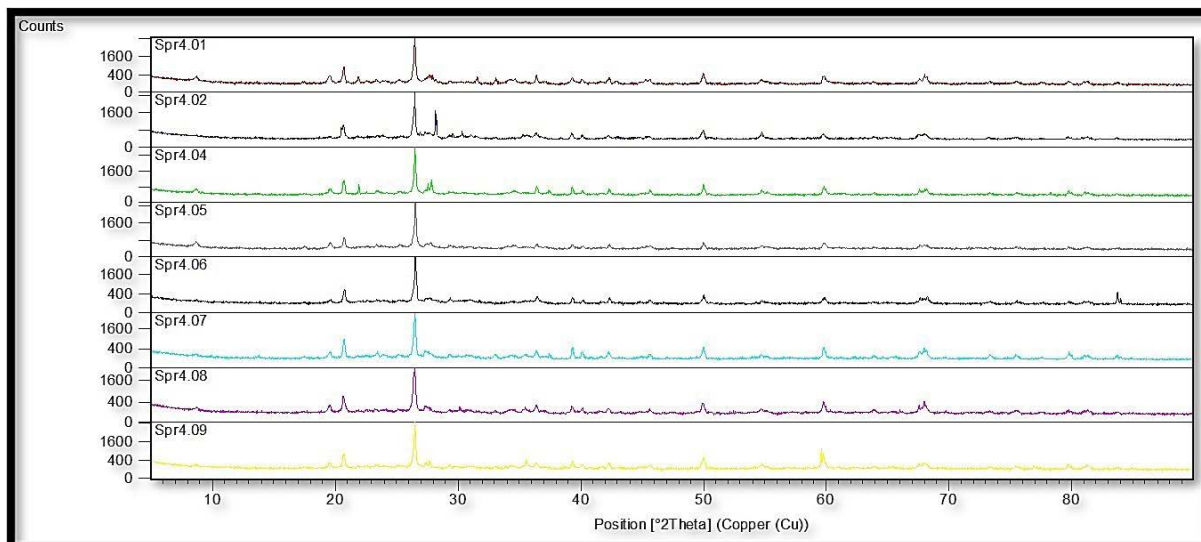


Figure 3d: XRD Graph of Singhpur (SPR) Site Samples (After: Geochronology Lab. IUAC. Delhi. India)

2593). Calcite is known to decompose completely at temperatures between 600 and 1000°C; however, it more commonly disappears within a narrower range of approximately 750–900°C (Gliozzo 2020: 8; Ion *et al.* 2023: 9–14; Seetha and Velraj 2019: 7). The presence of feldspar ($\text{NaAlSi}_3\text{O}_8$) indicates that firing temperatures may have reached 850°C or higher (Gliozzo 2020: 10–11).

Dolomite [$\text{CaMg}(\text{CO}_3)_2$] decomposes at temperatures between 800°C and 950°C (Yanik *et al.* 2012: 267). Biotite, a black mica, generally exhibits limited variation over the temperature ranges typically employed in ceramic firing, although decomposi-

tion begins at around 800°C. Riccardi *et al.* (1999) demonstrated that the optical properties of biotite first change at approximately 850°C, at which point it becomes opaque. Muscovite undergoes a progressive dehydroxylation process over a broad temperature range of approximately 800–1100°C (Hussin *et al.* 2018: 8–10; Viani *et al.* 2018: 114; Kurosawa *et al.* 2022: 14–15), with possible transformations to a spinel phase occurring at around 920°C (Hussin *et al.* 2018: 8). Depending on the chemical composition of illite, a wide variety of secondary phases may form within clay systems, including feldspar, hematite, and spinel (Yanik *et al.* 2012: 267).

The presence of hematite in the analysed samples suggests firing within a temperature range of approximately 400–850°C under oxygen-rich conditions (Gliozzo 2020: 34). Hematite is among the most potent colouring agents in pottery, with even small quantities, approximately 1–1.5%, being sufficient to impart a reddish hue to ceramic bodies (Velraj *et al.* 2010: 90). The occurrence of fluorine (CaF₂) indicates firing temperatures between 600 and 850°C (Garcia-Ten *et al.* 2006: 77–80; Dehne 1987: 9). Mica (phlogopite) begins to dehydroxylate at temperatures of approximately 850–900°C and continues to decompose up to 1100°C (Tutti *et al.* 2000: 601–603). Quartz, a non-clay mineral, is consistently present in all samples, and its survival suggests that firing temperatures did not significantly exceed approximately 1100°C (Ouahabi *et al.* 2015: 408).

Taken together, the mineralogical evidence points to a technologically dynamic ceramic tradition in the Jalandhar region. The coexistence of residual clay minerals alongside high-temperature phases indicates controlled yet varied firing practices. The partial preservation of carbonates and the transformation of mica minerals suggest firing within predictable thermal thresholds. While the present study relies primarily on XRD analysis, it is acknowledged that the absence of microstructural data limits direct observation of vitrification processes and amorphous matrix behaviour. Future integration of SEM–EDS analysis would allow for a more comprehensive assessment of microstructural evolution and firing mechanisms.

From a cultural and provenance perspective, the mineralogical data provide valuable insights into ancient technological choices and patterns of resource utilisation. Shifts in clay provenance observed at Kathpalon and Hardo Pharla, from Harappan and Medieval to Historical periods, may reflect changes in cultural groups or the reconfiguration of exchange networks. Such interpretations align with the principle that the provenance of ceramic artefacts is fundamentally linked to the selected clay sources and production locales. In this sense, each mineral assemblage functions as a geological and technological fingerprint of local craft traditions. For instance, the presence of specific accessory minerals in pottery from one period but not another suggests the exploitation of different raw material sources. At Goal Pind, the application of carbon-

blackening techniques in slips reflects specialised knowledge of reducing atmospheres and additives, a cultural practice documented in other ancient contexts. Overall, the present findings contribute significantly to our understanding of ancient ceramic technology in northern India and underscore the adaptability, skill, and accumulated knowledge of regional potters over millennia.

Conclusion

The ceramic assemblages from Kathpalon, Goal Pind, Hardo Pharla, and Singhpur consistently demonstrate evidence of controlled firing within a low to moderate temperature range, predominantly between 500°C and 900°C. Variations in mineralogical composition across cultural phases reflect both continuity and transformation in raw material selection and technological strategies.

This study underscores the value of XRD-based mineralogical analysis in reconstructing ancient ceramic traditions and highlights the dynamic nature of pottery production in the Jalandhar Doab region. By integrating scientific data with archaeological context, the research enhances our understanding of how ancient communities adapted their craft practices in response to changing cultural and environmental conditions.

Acknowledgement

Authors are thankful to IUAC for extending XRD facility funded by Ministry of Earth Sciences (MoES) under Geochronology project [MoES/P.O.(Seismic)8(09)-Geochron/2012]. Authors are also thankful to Dr. Pankaj Kumar and Leema Saikia for providing access to the XRD facility. Further, authors acknowledge the Indian Council of Historical Research (ICHR) for financial support for the field survey, and express sincere gratitude to Dr. Abdul Adil Pray from the Central University of Amarkantak, Madhya Pradesh, for his kind support. The authors are also grateful to the anonymous reviewers who reviewed this manuscript.

References

- Berry, L.G. (ed.). 1974. *Selected Powder Diffraction Data for Minerals*. Pennsylvania: Joint Committee on Powder Diffraction Standards.
- Bish, D. L. 1989. Modern Powder Diffraction. In J.E. Post, (ed.), *Reviews in Mineralogy and Geochemistry Series*. California: Mineralogical Society of America, 1-24.
- Cultrone, G; E. Molina; C. Grifa; E. Sebastian. 2011. Iberian Ceramic Production from Basti (Baza, Spain): First Geochemical, Mineralogical and Textural Characterization, *Archaeometry* 53(2): 340-363. <https://doi.org/10.1111/j.1475-4754.2010.00545.x>
- Dehne, G. 1987. Relationship between Fluorine Emission During Firing of Ceramic products and the Firing Temperature and Composition of Raw Material, *Applied Clay Science* 2(1): 1-9. [https://doi.org/10.1016/0169-1317\(87\)90010-X](https://doi.org/10.1016/0169-1317(87)90010-X)
- Garcia-Ten, J; E. Mofort; M.P. Gómez Tena & S. Gomar. 2006. Influence of Calcite Content on Fluorine Compound Emissions During Ceramic Tile Firing, *Journal of Ceramic Processing Research* 7(1): 75-82.
- Gliozzo, E. 2020. Ceramic Technology. How to Reconstruct the Firing Process, *Archaeological and Anthropological Sciences* 12(11): 260. <https://doi.org/10.1007/s12520-020-01133-y>
- Hussin, A; A.H.A. Rahman; K.Z. Ibrahim. 2018. Mineralogy and Geochemistry of Clays from Malaysia and its Industrial Application, *IOP Conference Series: Earth and Environmental Science*. 212(1): 012040 <https://doi.org/10.1088/1755-1315/212/1/012040>
- Ion, R.M; V. Diaconu; G. Vasilievici; L. Iancu; R.M. Grigorescu; L.A. Mirt; E. Alexandrescu; A.I. Gheboianu; S. Slamnoiu-Teodorescu. 2023. Archaeometric Investigations of the Chalcolithic Pottery from Topolit, a-Neamt, County. Romania. *Coatings* 13(1): 488. <https://doi.org/10.3390/coatings13030488>
- Kurosawa, M; M. Semmoto; T. Shibata. 2022. Mineralogical Characterization of Early Bronze Age Pottery from the Svilengrad-Brantiite Site, Southeastern Bulgaria, *Minerals* 12(1): 79. <https://doi.org/10.3390/min12010079>
- Ouahabi, El. M; L. Daoudi; F. Hatert; N. Fagel. 2015. Modified Mineral Phases During Clay Ceramic Firing, *Clays and Clay Minerals* 63(5): 404-413. <https://doi.org/10.1346/CCMN.2015.0630506>
- Rahul, 2024. Archaeological Explorations in the Adampur and Jalandhar East Blocks of Jalandhar District of Punjab: A Preliminary Report, *Quarterly Journal of The Mythic Society* 115: 26-35. <https://doi.org/10.58844/KZTT6011>
- Riccardi M.P; B. Messiga; P. Duminuco. 1999. An Approach to Dynamics of Clay Firing, *Applied Clay Science* 15(1): 393-409. [https://doi.org/10.1016/S0169-1317\(99\)00032-0](https://doi.org/10.1016/S0169-1317(99)00032-0)
- Seetha, D & G.Velraj. 2019. FT-IR, XRD, SEM-EDS, EDXRF and Chemometric Analyses of Archaeological Artifacts Recently Excavated from Chandravalli in Karnataka State, South India. *Radiation Physics and Chemistry* 162(1): 114-120. <https://doi.org/10.1016/j.radphyschem.2019.03.017>
- Tutti, F; L. Dubrovinsky; M. Nygren. 2000. High-temperature Study and Thermal Expansion of Phlogopite. *Physics and Chemistry of Minerals* 27(1): 599-603, <https://doi.org/10.1007/s002690000098>
- Velraj, G; R. Sudha; R. Hemamalini. 2010. X-Ray Diffraction and Tg-Dta Studies of Archaeological Artifacts Recently Excavated in Salamankuppam Tamilnadu, *Recent Research in Science and Technology* 2(10): 89-93.
- Viani, A; G. Cultrone; K. Sotiriadis; R. Ševčíka; P. Šašeka. 2018. The Use of Mineralogical Indicators for the Assessment of Firing Temperature in Fired-Clay Bodies, *Applied Clay Science* 163(1): 108-118. <https://doi.org/10.1016/j.clay.2018.07.020>

Wu, J; T. Houa; M. Zhanga; Q. Lia; J. Wua; J. Lib; Z. Denget. 2013. An Analysis of the Chemical Composition, Performance and Structure of China Yixing Zisha Pottery from 1573 AD to 1911 AD, *Ceramics International* 39(3): 2589-2595. <https://doi.org/10.1016/j.ceramint.2012.09.021>

Yanik, G; R. Bozer. M. Çeken; F. Esenli; H. Gocmez. 2012. The Characterization of Medieval Ceramics Excavated from the Eğirdir Caravanserai (Turkey), *Ceramics–Silikáty* 56(3): 261-268.